AGU PUBLICATIONS

JGR

Journal of Geophysical Research: Atmospheres

RESEARCH ARTICLE
10.1002/2015JD023159

Key Points:
- Link between preonset land atmospheric conditions and ISMR is explored
- This link will enhance our ability to predict monsoon in non-ENSO years
- Preonset rainfall/temperature variability is linked with stationary Rossby wave

Supporting Information:
- Figure S1
- Text S1

Correspondence to:
S. K. Saha,
subodh@tropmet.res.in

Citation:
Rai, A., S. K. Saha, S. Pokhrel, K. Sujith, S. Halder (2015), Influence of preonset land atmospheric conditions on the Indian summer monsoon rainfall variability, *J. Geophys. Res. Atmos.*, *120*, doi:10.1002/2015JD023159.

Received 27 JAN 2015
Accepted 21 APR 2015
Accepted article online 23 APR 2015

Influence of preonset land atmospheric conditions on the Indian summer monsoon rainfall variability

Archana Rai[1], Subodh K. Saha[1], Samir Pokhrel[1], K. Sujith[1], and Subhadeep Halder[2]

[1]Indian Institute of Tropical Meteorology, Pune, India, [2]Center for Ocean-Land-Atmosphere Studies, George Mason University, Fairfax, Virginia, USA

Abstract A possible link between preonset land atmospheric conditions and the Indian summer monsoon rainfall (ISMR) is explored. It is shown that, the preonset positive (negative) rainfall anomaly over northwest India, Pakistan, Afghanistan, and Iran is associated with decrease (increase) in ISMR, primarily in the months of June and July, which in turn affects the seasonal mean. ISMR in the months of June and July is also strongly linked with the preonset 2 m air temperature over the same regions. The preonset rainfall/2 m air temperature variability is linked with stationary Rossby wave response, which is clearly evident in the wave activity flux diagnostics. As the predictability of Indian summer monsoon relies mainly on the El Niño–Southern Oscillation (ENSO), the found link may further enhance our ability to predict the monsoon, particularly during a non-ENSO year.

1. Introduction

The year-to-year variability of Indian summer monsoon rainfall (ISMR) has a large impact on the economy and agriculture of the country. A large part of the population depends on agriculture, which is mostly rainfed. Therefore, accuracy in the prediction of ISMR has an immense importance, which can help the society to manage with the adverse effect of the monsoon, particularly the drought condition. The interannual variability (IAV) of ISMR is mainly associated with variations in sea surface temperatures (SSTs) over the equatorial Pacific (i.e., El Niño–Southern Oscillation (ENSO)) [*Sikka*, 1980; *Rasmusson and Carpenter*, 1983; *Krishna Kumar et al*., 1999] and over the Indian Ocean (i.e., Indian Ocean Dipole Mode (IOD)) [*Saji et al*., 1999]. Apart from SST, land surface variability such as Eurasian snow cover also influences the IAV of ISMR [*Bamzai and Shukla*, 1999; *Kripalani and Kulkarni*, 1999; *Saha et al*., 2013]. So far, we have mainly relied on ENSO and to some extent on IOD for the predictability of ISMR. Almost all the statistical seasonal prediction models of monsoon rainfall depend on the change in magnitude of different ENSO indices [*Shukla and Paolino*, 1983]. However, the Indian summer monsoon is a land-ocean-atmosphere coupled system, and some predictability may arise from better understanding of land-atmosphere coupled processes and their incorporation into the forecast system.

Total rainfall in a monsoon season (June-July-August-September; JJAS) is a measure of performance of the monsoon of that year. According to the India Meteorological Department (IMD), a year is a "normal monsoon year" when the all-India averaged seasonal (JJAS) rainfall is within ±10% of its long-term average. However, IAV of monthly rainfall is also quite large. For example, heavy rainfall in the months of June and July may be followed by relatively dry conditions in the following two months and vice versa, which may sometimes result into a normal monsoon year [*Kothawale and Kulkarni*, 2014]. Since the prediction of seasonal rainfall provides an overall view of the monsoon, advanced information about the space-time distribution of rainfall is the most sought input for agricultural and other planning. For example, the year 2012 was a normal (93%) monsoon year, but the whole country was very dry during the entire month of June and part of July. The averaged rainfall over all-India in the months of June, July, August, and September was 72, 87, 101, and 112% with respect to its long-term mean [*Pai and Bhan*, 2013]. It is also observed that in the year 2012, Niño3.4 SST anomaly was very weak. The Niño3.4 SST averaged over the months March-April-May, April-May-June, May-June-July, June-July-August, and July-August-September was −0.3, −0.2, 0.0, 0.1, and 0.4°C, respectively (http://www.cpc.ncep.noaa.gov/products/analysis\monitoring/ensostuff/ensoyears.shtml). There was abrupt development of positive IOD mode in the Indian Ocean during July–August 2012, which enhanced the rainfall in the last half period of the monsoon [*Pai and Bhan*, 2013]. However, still it is not clear that why the months of June and part of

July were so dry? This motivates us to look for processes/predictors other than ENSO and IOD for more accurate space-time prediction of ISMR.

Diabatic heating over the Tibetan Plateau [*Abe et al*., 2003] and moist land surface processes, including vegetation [*Prasanna and Yasunari*, 2009; *Takata et al*., 2009], help the monsoon rainfall to penetrate into deep interior of the continent and also make the monsoon vigorous. Soil moisture possesses memory and its nonlinear interactions with vegetation and atmosphere may also enhance the effective memory by up to several months [*Walsh et al*., 1985; *Shinoda and Gamo*, 2000]. Since there are very few long term in situ measurements of soil moisture over the monsoon region [*Robock et al*., 2003]; therefore, it is difficult to demonstrate monsoon predictability arising from land-atmosphere coupled processes. Another way to demonstrate the influence of land-atmosphere processes on the monsoon is through state-of-the-art numerical models. Many previous modeling studies have recognized land-atmosphere interactions as one of the important source of monsoon variability [*Shukla and Mintz*, 1982; *Webster*, 1983; *Meehl*, 1997; *Ferranti et al*., 1999; *Koster et al*., 2004]. Modeling studies have also shown that soil moisture variability over semiarid region has stronger effect on rainfall than that of wet region [*Douville et al*., 2002; *Koster et al*., 2004]. Northwest region of India shows largest rainfall variability associated with soil moisture [*Koster et al*., 2004]. Since the soil moisture memory varies from weeks to several months, it is plausible to improve the prediction skill not only on the seasonal time scale but also on the intraseasonal time scale [*Ferranti et al*., 1999; *Saha et al*., 2012]. Furthermore, a significant part of IAV of ISMR may arise due to premonsoon land surface processes and their interaction with climatological intraseasonal oscillation. This is part of internal variability, which arises from regional (central India) land-atmosphere feedback [*Saha et al*., 2011]. However, there might be large-scale signal in terms of stationary/quasi-stationary land atmospheric mode, which is independent of ENSO and may affect the following monsoon rainfall. Therefore, in non-ENSO year, the first phase of ISMR variability caused by land-atmosphere interactions may be predictable in advance (weeks to months).

In the present study, it is shown that IAV of preonset (April and May) rainfall and surface temperature over northwest region of India is strongly linked with the rainfall of following monsoon months (particularly in the month of June and July) and contributes significantly to the ISMR. This finding may have implications in terms of improving forecast skill of June and July rainfall and hence the seasonal monsoon rainfall. The data sets used in this study and the method of analysis are described in section 2. Results are discussed in section 3, and possible mechanisms are given in section 4. Section 5 describes the summary.

2. Data and Methods

Asian precipitation-highly resolved observational data integration toward evaluation (APHRODITE) water resources daily rainfall data (0.5° × 0.5°) for the period 1951–2007 is used (http://www.chikyu.ac.jp/precip/index.html). The APHRODITE project has developed state-of-the-art daily precipitation data sets with high-resolution grids for Asia. The data set was created primarily with data obtained from a rain gauge observation network [*Yatagai et al*., 2012]. Apart from APHRODITE rainfall data, Global Precipitation Climatology Project (GPCP) version 2 [*Adler et al*., 2003] monthly rainfall (2.5° × 2.5°, 1979–2007), IMD-generated [*Rajeevan et al*., 2006] gridded daily rainfall (1° × 1°, 1951–2007), and the Tropical Rainfall Measurement Mission Project (TRMM) 3B42v7 [*Huffman et al*., 2007] daily rainfall (0.25° × 0.25°, 1997–2007) are also used in this study. National Oceanic and Atmospheric Administration (NOAA) outgoing longwave radiation (OLR) monthly data [*Liebmann and Smith*, 1996] (2.5° × 2.5°, 1979–2007) are used as a proxy of rainfall. Since the climatological onset of Indian summer monsoon over Kerala (southern tip of India) is 1 June, April to May is considered as preonset period throughout the analysis. For the representation of rainfall over India, area-averaged rainfall over central India (CI; 70°–90°E, 12°–30°N) is used, which is slightly bigger than homogeneous rainfall area as defined by *Goswami et al*. [2006]. High-resolution (0.5° × 0.5°) gridded 2 m monthly air temperature data CRU TS 3.1 is obtained from the Climatic Research Unit (CRU), University of East Anglia, for the period 1951–2007 [*Harris et al*., 2014]. Multimodel averaged daily soil moisture data (1° × 1°) from Global Soil Wetness Project-2 (GSWP-2) [*Dirmeyer et al*., 2006] from 1986 to 1995 are used for calculating the soil memory. The Pearson correlation coefficient is used to quantify the linear association between the preonset rainfall/temperature and following monsoon month rainfall.

To demonstrate the large-scale circulation and the wave activity flux associated with the preonset rainfall, monthly data for zonal (u), meridional (v) wind, geopotential height, and air temperature for the period

1948–2000 are obtained from National Centers for Environmental Prediction/National Center for Atmospheric Research (NCEP/NCAR-I) reanalysis [*Kalnay et al.*, 1996]. Extended Reconstructed SST (ERSST) version 3b data for the period 1951–2007 [*Smith et al.*, 2008; *Reynolds et al.*, 2002] is used to identify ENSO years. ENSO years are classified according to the definition used by the U.S. National Weather Service (http://www.cpc.ncep.noaa.gov/products/analysis_monitoring/ensostuff/ensoyears.shtml). Niño3.4 index is calculated by taking area-averaged SST over 5°N–5°S, 120°W–170°W. The year with JJAS averaged Niño3.4 SST above 0.5°C and below −0.5°C is considered as an ENSO year.

The wave activity flux [*Takaya and Nakamura*, 2001] is calculated for representing three-dimensional propagation of stationary/quasi-stationary waves in the zonally asymmetric basic state. Its expression in the logarithm pressure coordinate is given as

$$W = \frac{p}{2|U|}\begin{bmatrix} U\left(v'^2 - \psi' v'_x\right) + V\left(-u'v' + \psi' u'_x\right) \\ U\left(-u'v' + \psi' u'_x\right) + V\left(u'^2 + \psi' u'_y\right) \\ \frac{f_0 R_a}{N^2 H_0}\left\{U\left(v'T' - \psi' T'_x\right) + V\left(-u'T' - \psi' T'_y\right)\right\} \end{bmatrix}$$

where ψ' denotes perturbation geostrophic stream function, T' perturbation temperature, (u', v') perturbation geostrophic velocity, (U, V) the geostrophic basic-flow velocity, R_a the gas constant of dry air, H_0 the constant scale height, p the normalized pressure, and N the Brunt-Väisälä frequency defined for the basic flow. The data sets are monthly gridded fields of winds, geopotential height, and temperature at 200 hPa level from NCEP/NCAR-I reanalysis. In this study, monthly data field is considered as the basic state in which quasi-stationary waves are embedded, and the anomalies are regarded as fluctuations associated with those waves. This diagnostic, denoted as W, is a three-dimensional vector which can be interpreted in the context of linear quasi-geostrophic dynamics. The flux is parallel to the local three-dimensional group velocity of stationary Rossby waves. The phase-independent flux (W) is suitable for a snapshot analysis of stationary or migratory Rossby wave on a zonally varying basic flow [*Takaya and Nakamura*, 2001]. Nonzero $\nabla \cdot W$ represents the sources (positive divergence) and sinks (negative divergence) related to wave activity. These wave "sources" or "sinks" are important tool for identifying the dynamics behind various atmospheric phenomena related to wave-mean flow interaction, nonlinearity, transient forcing, and nonconservative physics such as heating and friction.

3. Results

About 40% of the interannual variance of ISMR during 1860–1980 can be explained by the ENSO. However, in recent decades, the relation between ENSO and ISMR has become significantly weaker [*Krishna Kumar et al.*, 1999]. Therefore, the obvious question is what are the other sources of ISMR variability? Is there another stationary or quasi-stationary mode of variability associated with land and atmosphere, which affects the ISMR variability? In this study, the possible stationary or quasi-stationary modes of land and atmospheric variability during premonsoon season and their effects on the ISMR are explored.

3.1. Relation Between Preonset Rainfall/Temperature and ISMR

In order to establish a link between preonset land surface condition and the following monsoon rainfall, the most sought land surface parameter is the soil moisture at deeper levels (i.e., few centimeters from the surface to 1 m depth/root zone depth). This is because land surface retains memory primarily in the form of available soil moisture, which is caused by rainfall or snowmelt in the past. Therefore, rainfall may also be considered as a proxy of soil moisture. On the other hand, preonset rainfall variability is also linked with the large-scale atmospheric circulation pattern, which is again coupled with ocean and land. Therefore, the question arises whether a preonset mode of variability exists and that affects the following monsoon rainfall and hence can be used to enhance the ISMR predictability. If such relationship between the preonset mode of variability and the following monsoon months rainfall exists, it can be seen in the correlation between rainfalls of these periods.

Figures 1a–1c show the correlation between the preonset rainfall at each grid point and area-averaged rainfall over central India for the months of June, June-July, and June-July-August, respectively, using the APHRODITE data for the period 1951–2007. A strong and significant negative (positive) correlation is observed over northwest India, which is extended toward Pakistan, Afghanistan, and part of Iran (northeast India and Myanmar) in the month of June, June-July, and June-July-August. Gradual decrease in correlation suggests

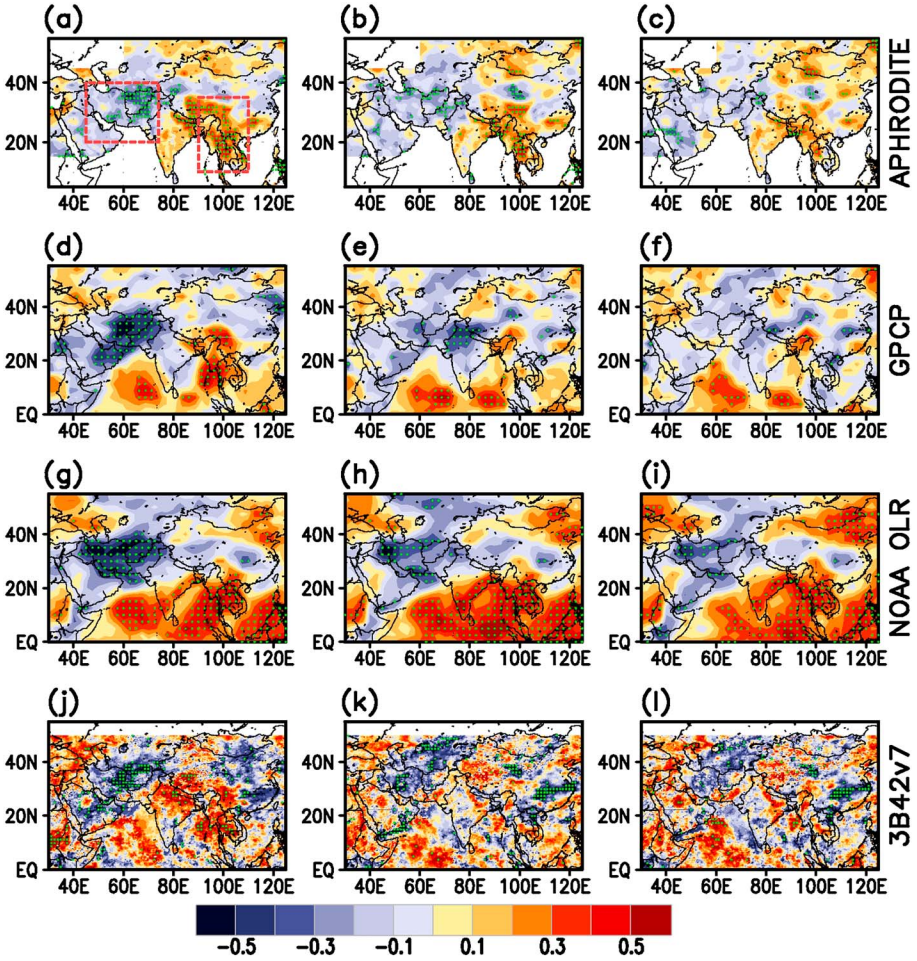

Figure 1. Correlation between preonset (April and May) rainfall (mm/d, APHRODITE data) at each grid and area-averaged rainfall over central India (CI; 70°–90°E, 12°–30°N, APHRODITE data) for (a) June, (b) June to July, and (c) June to August. (d–l) The same as above but for GPCP (Figures 1d–1f), NOAA OLR (Figures 1g–1i), and TRMM 3B42v7 (Figures 1j–1l) data sets. The green dots represent the correlation significant at 95%. The red boxes in northwest and southeast of India show the regions, which are used for constructing preonset rainfall index.

that the relation is much stronger in the month of June and then decreases its strength with time. In order to establish whether this relation is consistent with other independent data, the same correlation is derived using rainfall data from GPCP and TRMM 3B42v7 as well as OLR data from NOAA (Figures 1d–1l). All of the above data sets reveal similar correlation pattern to that of APHRODITE, but their amplitudes are different. The reason of such differences in amplitude is that all the data sets have been developed using different input sources, and the time span of these data sets is also not similar. The APHRODITE rainfall data are based on rain gauge observation network, while GPCP rainfall data are merged product, based on satellite and rain gauge observations. TRMM rainfall data are purely based on satellite observations. From GPCP rainfall and NOAA OLR, it is evident that the positive correlation over southeast region is extended over the oceanic regions of Bay of Bengal (BoB) and the Arabian Sea around 10°N. Therefore, an increased preonset rainfall over the northwest (southeast) region is associated with decreased (increased) postonset rainfall over India, and this relation becomes weaker after the first 2 months (June and July). The correlation pattern obtained from IMD-gridded rainfall data (Figure S1) is similar to the above mentioned data sets (Figure 1) and is highly significant, particularly over northwest and east India region. Recently, *Prakash et al.* [2014] reported that APHRODITE is the most reliable rainfall data among six different gridded data sets (GPCP, CRU, Climate Prediction Center Merged Analysis of Precipitation (CMAP), Climate Prediction Center (CPC), Global Precipitation Climatology Center (GPCC), and APHRODITE). Therefore, the relationship between preonset and area-averaged rainfall from the APHRODITE data set is likely to be robust.

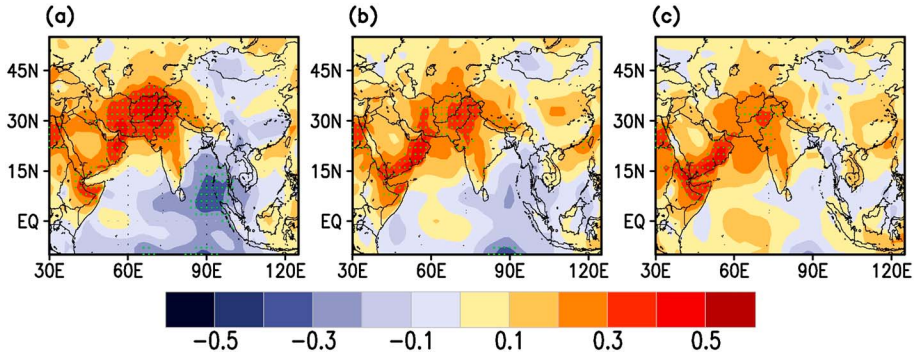

Figure 2. Correlation between preonset (April and May) 2 m air temperature (°C, CRU TS 3.21 data over land), SST (°C, ERSST over ocean) at each grid and area-averaged rainfall (mm/d, APHRODITE) over central India (70°–90°E, 12°–30°N) for (a) June, (b) June to July, and (c) June to August. The green dots represent the correlation significant at 95%.

The very basic theory of monsoon, long ago proposed by *Halley* [1686], is based on land-sea breeze concept. The large-scale meridional surface temperature gradient develops due to different heat capacity of land and adjoining ocean through the seasonal cycle of solar heating during boreal spring [*Li and Yanai*, 1996]. This helps in the formation of surface heat-low during late spring. Therefore, the preonset land surface temperature is also expected to be warmer (colder) for the years with excess (deficit) rainfall during the first phase of the monsoon (i.e., June and July). In order to examine this relation, correlation between preonset 2 m air temperature/SST at each grid point and the monsoon rainfall area-averaged over CI is calculated for the month of June, June-July, and June-July-August. CRU TS 3.21, ERSST, and APHRODITE data are used for surface temperature, SST, and rainfall, respectively, for the period 1951–2007 to derive the correlation. A strong and significant positive (negative) correlation between preonset 2 m air temperature/SST and the monsoon rainfall area averaged over CI is evident over northwest India, Pakistan, Afghanistan, and Iran (southeast region and BoB) (Figure 2). Furthermore, this relation is strongest for CI rainfall for the month June and gradually becomes weaker/insignificant for June-July, and June-July-August. Thus, the above correlations clearly suggest that there exists a strong and an inverse relation between the preonset rainfall over southeast region (including BoB) and the heat-low region. In fact, the correlation between preonset (April and May) rainfall over a box (45°–74°E, 20°–40°N) in the heat-low region and southeast region (90°–110°E, 10°–35°N), using APHRODITE data (1951–2007), is −0.45, which is significant above the 99% level. This suggests that preonset surface conditions over southeast including BoB (which is also a part of early phase of the East Asian summer monsoon) and the heat-low regions are dynamically linked through the atmosphere.

3.2. Composite Analysis

In order to scrutinize the link between preonset rainfall over the heat-low region and the following monsoon rainfall in a quantitative way, composite analysis is carried out. Preonset rainfall index is calculated based on normalized April and May rainfall anomaly over a box (45°–74°E, 20°–40°N; shown in Figure 1) in the heat-low region using APHRODITE rainfall data. The rainfall anomaly is normalized with its own standard deviation (SD). For the composite analysis, we assume that stronger preonset rainfall anomaly (i.e., ±1 SD) will have clear signal/response on the following monsoon rainfall. However, to increase the number of samples, ±0.8 SD is chosen as the lower limit for strong anomaly year (Figure 3a). Some of these strong years are also ENSO year (represented by cross mark in Figure 3a). ENSO is a major modulating factor of year-to-year variability of rainfall over the Indian region. Therefore, to find out how much the rainfall anomaly is due to the processes other than ENSO, ENSO years are excluded from the composite analysis. The year with preonset rainfall anomaly ≥ 0.8 SD is considered as Positive Rainfall Anomaly (PRA) year, and the year with preonset rainfall anomaly ≤ -0.8 SD is considered as Negative Rainfall Anomaly (NRA) year, respectively. Using the above criteria, 9 years (1957, 1962, 1968, 1969, 1976, 1983, 1992, 1993, and 1995) are identified as PRA year and 8 years (1958, 1959, 1978, 1980, 1984, 1989, 2000, and 2001) are identified as NRA year.

3.2.1. Rainfall

Figure 3b shows the evolution of composite of accumulated rainfall anomaly (using APHRODITE rainfall data) over CI for NRA and PRA years. It is evident that changes in rainfall are large and significant during the month

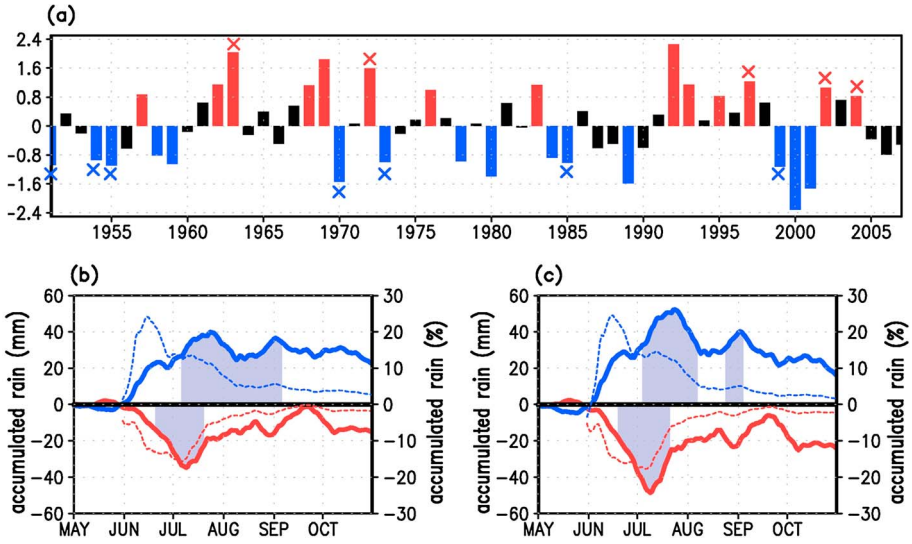

Figure 3. (a) Preonset (April and May) rainfall anomaly averaged over the heat-low region (northwest box in Figure 1) using APHRODITE data. Rainfall anomaly is normalized by its own standard deviation. Cross marks represent the ENSO years. (b) The composites of CI averaged accumulated rainfall anomaly for the non-ENSO and stronger preonset rainfall year (northwest box averaged rainfall anomaly ≥ 0.8 and ≤ -0.8 from Figure 3a). Blue (red) solid curve represents the composite (in mm) based on negative (positive) northwest box rainfall anomaly years. The dotted blue and red lines are the same as the corresponding solid lines, but in percentage with respect to climatological mean accumulated rainfall (right *y* axis). (c) Same as Figure 3b but using IMD-gridded rainfall data. The shaded regions are significant at 95%.

of June and July (by maximum of about 20% of the accumulated rainfall). After July, the rainfall anomaly tends to come closer to the climatological mean, particularly for PRA years. Therefore, at the end of a season, the accumulated seasonal rainfall may be near normal, but in reality it may cause strong flood/drought conditions in the beginning of the monsoon season, which has large economic and societal impacts. Figure 3c also depicts the same, but the composite of accumulated rainfall anomaly is derived from IMD-gridded rainfall data. The conformity of the finding, using two independent data sets, ensures the robustness of the result.

3.2.2. Low-Level Atmospheric Circulation

The basic feature of the monsoon is characterized by the southeasterly winds in the southern Indian Ocean, which crosses the equator and becomes southwesterly in the northern tropical Indian Ocean. These winds bring ample moisture from the warm water of the tropical ocean to the Indian subcontinent. During the summer monsoon season, a low-level strong westerly jet is observed over the Arabian Sea, known as Findlater Jet [*Findlater*, 1969], which peaks at around Somali coast.

In order to see how the preonset rainfall over the heat-low region modifies the large-scale circulation during PRA and NRA years, composite of low-level wind (850 hPa) anomalies during PRA and NRA years for preonset (April and May), June, July, and August are constructed using NCEP/NCAR-I wind data and shown in Figure 4. It is evident from Figure 4 that the PRA years (in the months of June, July, and August) are associated with a weakening of the westerly monsoon flow into India from the Arabian Sea. Contrary to PRA years, NRA years reveal a stronger low-level southwesterly jet over the Arabian Sea. In NRA years, wind anomalies are much stronger in the months of June and July, which in turn increase the moisture flux and hence lead to wetter condition over the Indian land region. It is also observed that wind anomalies (both in the composite of PRA and NRA years) are stronger in June and July and then the strength of the anomalies decrease. Therefore, decrease (increase) in the rainfall during PRA (NRA) years is associated with decrease (increase) in the mean monsoon circulation.

3.2.3. Tropospheric Temperature

The north-south tropospheric temperature gradient (TTG) is one of the important parameters related with the onset and withdrawal of the monsoon [*Ueda and Yasunari*, 1998]. Tropospheric temperature (TT) is defined as the vertically averaged air temperature between 200 hPa and 600 hPa [*Goswami and Xavier*, 2005]. The meridional TTG is also important for sustaining the monsoon circulation. In order to see how the preonset

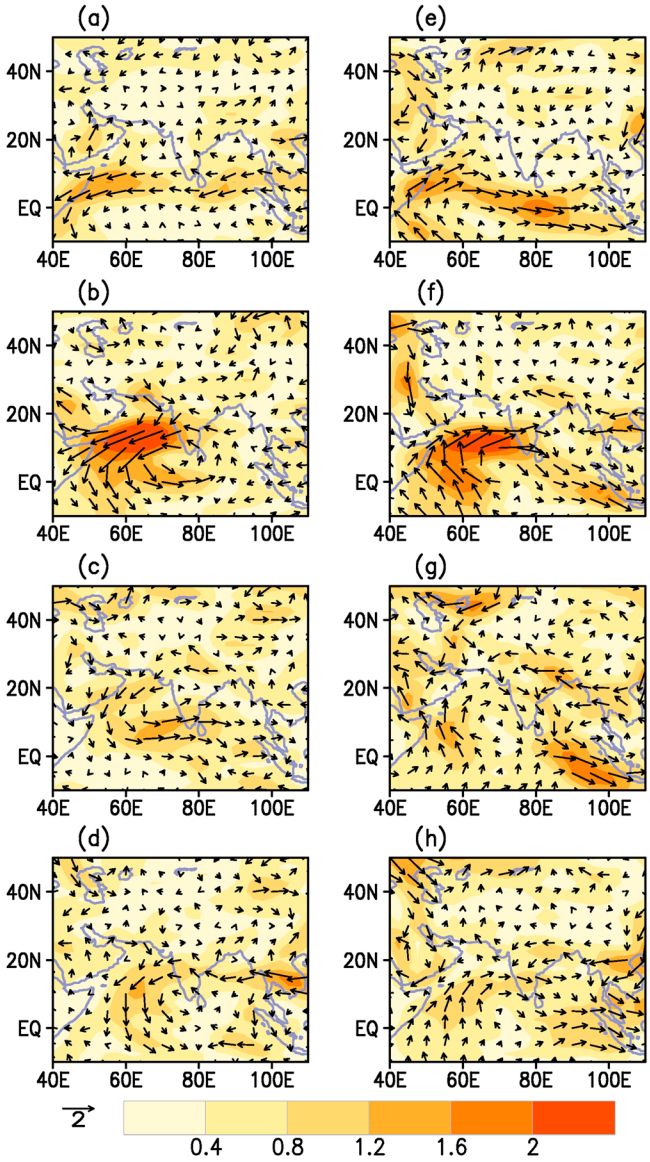

Figure 4. Composite of wind anomalies (m s^{-1}) at 850 hPa for (a–d) PRA and (e–h) NRA years in preonset, June, July, and August, respectively. The shading represents the magnitude of wind, and the arrow represents the direction.

rainfall variability is associated with TTG, composite difference of TT between NRA and PRA years for preonset, June, July, and August, is constructed using NCEP/NCAR-I air temperature (Figure 5).

It is observed that difference in TT is large and positive during preonset (April and May), June, and July over the northern part (north of 20°N), nevertheless during August it is relatively small. This implies that TTG is large during NRA years as compared to the PRA years, which is favorable condition for the monsoon rainfall. The buildup and maintenance of TT is the key process in linking the heat-low region and ISMR, and this link may be associated with land-atmosphere interactions. Furthermore, enhanced (decreased) TTG is associated with increased (decreased) rainfall over east and southeast of Indian subcontinent during preonset, which again happens to be the beginning phase of East Asian Monsoon. It is interesting to note that preonset rainfall is associated with large-scale phenomena like TT, which suggests the existence of large-scale mode of variability during preonset season.

4. Possible Mechanisms

The findings discussed in the previous section suggest that the signal persists primarily from premonsoon up to the month of July, which causes significant changes in the ISMR. As the atmosphere, ocean, and land are intimately coupled with each other in a complex fashion; therefore, it is challenging to find out the mechanism for a variability/change in climatic parameter. However, we seek of linear relations, which can be used for improving weather/climate prediction. As in the composite analysis, we have discarded ENSO years, the found ISMR variability is independent of ENSO. However, preonset rainfall variability may be linked with ENSO and thus can have an indirect effect. Regional land atmospheric feedback during preonset period may also causes memory through soil moisture, which can affect the monsoon circulation. Ultimately, a signature of stationary mode may be evident in the atmosphere, which connects preonset to postonset monsoon period. Therefore, finally we diagnose existence of stationary/quasi-stationary waves in terms of wave activity flux.

4.1. ENSO and Preonset/Postonset Rainfall

Now to examine whether the preonset rainfall over the heat-low region has any link with ENSO and how all above relations are evolved with time, sliding correlation is used. Sliding correlation gives the changes of strength of correlation with time. Sliding correlation can be useful for evaluating the temporal

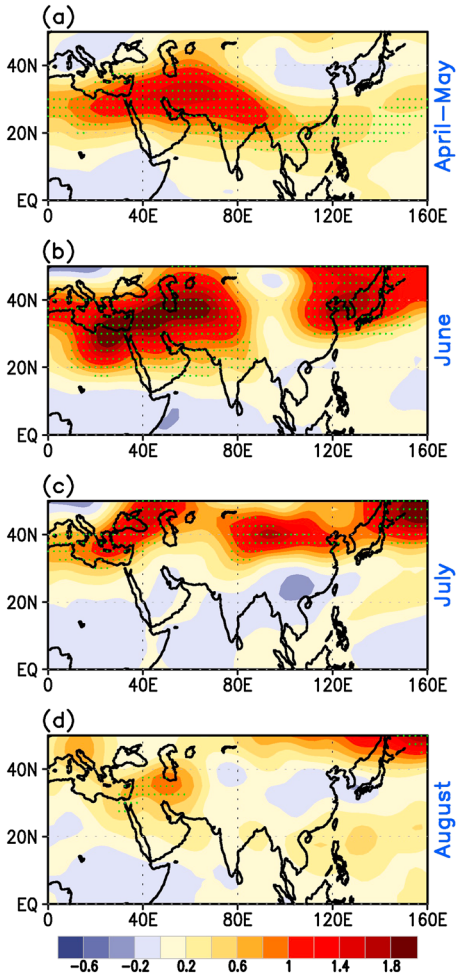

Figure 5. Composite difference of NRA and PRA years tropospheric temperature (°C, air temperature averaged over 200–600 hPa) for (a) preonset (April and May), (b) June, (c) July, and (d) August.

change in strength of relationship quantitatively. In general, time window of 30 years is considered to be reasonable to represent climatology of a meteorological parameter. Therefore, it is possible to evaluate changes in the climatic relationship between two parameters having record length greater than 30 years. However, sliding correlation on a 21 year moving window is also used in many previous study [e.g., *Krishna Kumar et al.*, 1999] to demonstrate changing climatic relationship. Correlation using data of first 21 year window (1951–1971) is calculated and that represents correlation value of 1961. The next time window is shifted by 1 year (i.e., 1952–1972), and the correlation value assigned for year 1962 and so on. Thus, there are 37 correlation values (1961–1997) using 21 year sliding window on data of 57 year (1951–2007), which depicts the changing relation between two parameter during 1961–1995. In this subsection, APHRODITE rainfall and ERSST data are used to derive sliding correlation. Sliding correlation (21 year window) between preonset rainfall over the heat-low region and Niño3.4 SST (April and May) shows that the correlation is always positive, and it has become stronger and significant (95%) after 1980 (Figure 6a). On the other hand, correlation between rainfall over India and Niño3.4 SST during June is very weak and not significant after 1965 (Figure 6c). However, the relation between Niño3.4 SST and rainfall over India is stronger during the last half part of the monsoon season (i.e., August to September). It may be noted that ISMR-ENSO relation has become weaker [*Krishna Kumar et al.*, 1999] after 1982–1983, which is also evident in Figure 6c. These correlations clearly suggest that ENSO does not have substantial influence on the starting phase (i.e., June and July), rather it dominates the later phase of monsoon. However, the preonset rainfall variability over the heat-low region is strongly linked with the starting phase of monsoon rainfall.

The correlation between preonset rainfall over the heat-low region and rainfall over India is also not stationary (Figure 6b). It is evident that preonset rainfall over the heat-low region and India is poorly correlated. However, the correlation between preonset rainfall over the heat-low region and rainfall over India during May and June becomes strong and is significant throughout the data period. Gradual decrease in the relation between preonset rainfall of heat-low region and following June-July and July-August rainfall over India is also evident throughout the entire data period.

To find out whether there is a link between simultaneous rainfall over the heat-low region and India and their time evolution, sliding correlation (21 year window) is calculated. It is interesting to note that there is no significant correlation between rainfall over the heat-low region and India for simultaneous period of April–May and May–June. During June-July and July-August, the rainfall over India and heat-low region is always positively correlated (significant at 95%; Figure 6d). This is because the onset of monsoon over northwest

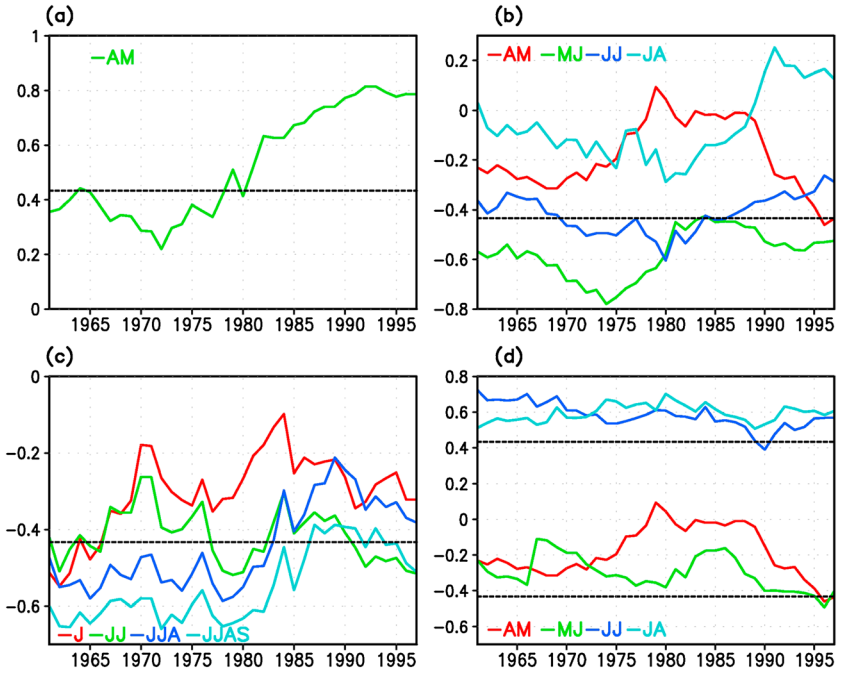

Figure 6. Sliding correlation (21 year window) between (a) preonset (April and May) rainfall (mm/d) over northwest box (in Figure 1) and Niño3.4 SST (°C, April and May), (b) preonset rainfall over northwest box and CI averaged rainfall of April-May, May-June, June-July and July-August. (c) Niño3.4 SST and CI averaged rainfall of the months June, June-July, June-July-August, and June-July-August-September, respectively. (d) Sliding correlation between rainfall averaged over northwest box and CI for simultaneous periods of April–May, May–June, June–July, and July–August, respectively. The black dashed line represents the significance level at 95%.

India generally takes place in the month of July, and the convective system, which forms over BoB, moves toward west and causes rainfall over there. The correlation between rainfall for two consecutive monsoon months over India is also not significant. It may be noted that main conclusions drawn here, based on sliding window of 21 year, do not change even a sliding window of 31 year is used (figure not shown).

4.2. Soil Moisture Memory

Northwest India, Pakistan, Afghanistan, southeast Arabia, and Iran are primarily arid/semiarid regions and maintain deep low during spring and summer [*Ramage*, 1966; *Rodwell and Hoskins*, 1966; *Sikka*, 1997; *Bollasina and Ming*, 2013]. Mean sea level pressure over northwest India during spring is inversely related with the following monsoon rainfall [*Parthasarathy et al.*, 1992; *Singh et al.*, 1995]. The climatological mean preonset OLR has large values over the heat-low, which is primarily a cloud-free region (Figure 7c). The mean preonset rainfall and variability (Figure 7e) are also consistent with OLR over this region. The interannual coefficient of variation (COV; defined as the ratio of SD to the mean) of rainfall is very large (Figures 7d and 7f) over the heat-low region. In fact, OLR is a good proxy of rainfall; and therefore, larger SD in OLR over the heat-low region (figure not shown) indicates larger variability in rainfall. However, SD of rainfall over the heat-low region is very small as compared to that of other part of the domain shown here. This is because rainfall follows the Poisson's distribution; and hence, large SD is colocated with large mean. Therefore, the rainfall variability in terms of SD may undermine its importance over the heat-low region as compared to other heavy rainfall region (i.e., eastern part of India). To overcome this problem, COV rather than SD is presented here. It is evident that IAV of rainfall is in the order of its seasonal mean. Therefore, the heat-low region experiences extreme changes (with respect to its mean state) in the surface energy and water balance. The IAV of rainfall is often associated with intraseasonal rainfall variability [e.g., *Goswami and Ajayamohan*, 2001]. Therefore, an extreme season (dry/wet) may be the result of some extreme (or many moderate) weather events.

The anomaly in the soil moisture is likely to have persistence of several days to several months, which may cause climate memory through anomalous surface energy and moisture fluxes. The wet and dry conditions

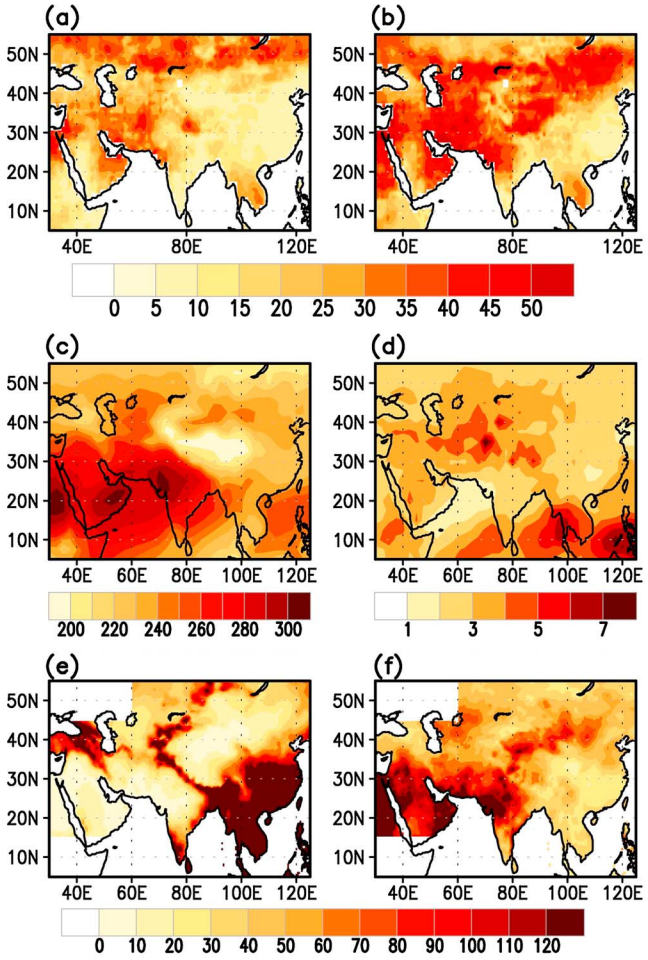

Figure 7. Soil memory (in days) using GSWP-2 soil moisture during preonset (April and May) at (a) 10 cm depth and at (b) 70 cm depth. (c) Climatological mean and (d) interannual coefficient of variation (in %) of preonset NOAA OLR. (e) Climatological mean and (f) interannual coefficient of variation (in %) of preonset rainfall from APHRODITE.

can be remembered by the soil, which is termed as soil memory. The length of soil memory is calculated by means of autocorrelation. Autocorrelation is computed at each grid point at 10 cm and 70 cm depths. The lag day, when autocorrelation of soil moisture drops below 95% significance level, is considered as length of memory.

Autocorrelation of preonset soil moisture at 10 cm and 70 cm depths from GSWP-2 data shows that correlation decreases below 95% significance level after 30–40 days over the heat-low region (Figures 7a and 7b). Therefore, it is plausible that soil moisture retains memory on above time scale and causes change in the surface energy balance. As soil moisture retains memory, the coupled land-atmosphere interactions may also enhance the persistence of anomalous low over the heat-low region and may affect the early ISMR.

4.3. Effects of Stationary/Quasi-Stationary Waves (Wave Activity Flux)

The wave activity flux (W) is used to diagnose the net effect of stationary Rossby waves at all the wave numbers [*Takaya and Nakamura*, 1997, 2001]. This is an extension of zonally averaged Eliassen-Palm flux to nonzonally averaged flows. The wave activity flux is parallel to the local group velocity; and hence, vectors depict the direction of Rossby wave raypaths. In low latitudes, quasi-geostrophic assumption breaks down, leading to very large amplitude and meaningless results for W. Therefore, the wave activity flux is calculated over the region above 10°N and for preonset, June, July, and August. In order to find out source and sink regions, horizontal divergence of W ($\nabla \cdot W$) is calculated.

In general, the amplitude of wave activity flux is larger in the composite of NRA years as compared to that of PRA years (Figure 8). The wave activity flux is higher during preonset to June and then decreases in the following months. Furthermore, the region of maximum wave activity flux moves northward progressively with the season. This is again consistent with the gradual northward shift of the position of the subtropical jet (figure not shown), which acts as a waveguide for stationary eddies. In July and August, the wave activity is confined only in the midlatitudes (north of 30°N) and not over the Indian land region. It is interesting to note that W and TTG have common spatial extent and shift in the position of their respective maxima. Therefore, buildup of TTG during preonset and in the following months is associated with stationary Rossby wave activity. In the composite of NRA years, the wave activity flux shows a major source of stationary wave activity between 30–60°E with zonal propagation toward the heat-low and Indian land region along 20–30°N during preonset. The flux source regions may indicate forcing from the midlatitudes and arid/semiarid region. The location of stationary wave activity source coincides with the position of subtropical jet and suggests that the forcing mechanism may be associated with instability in

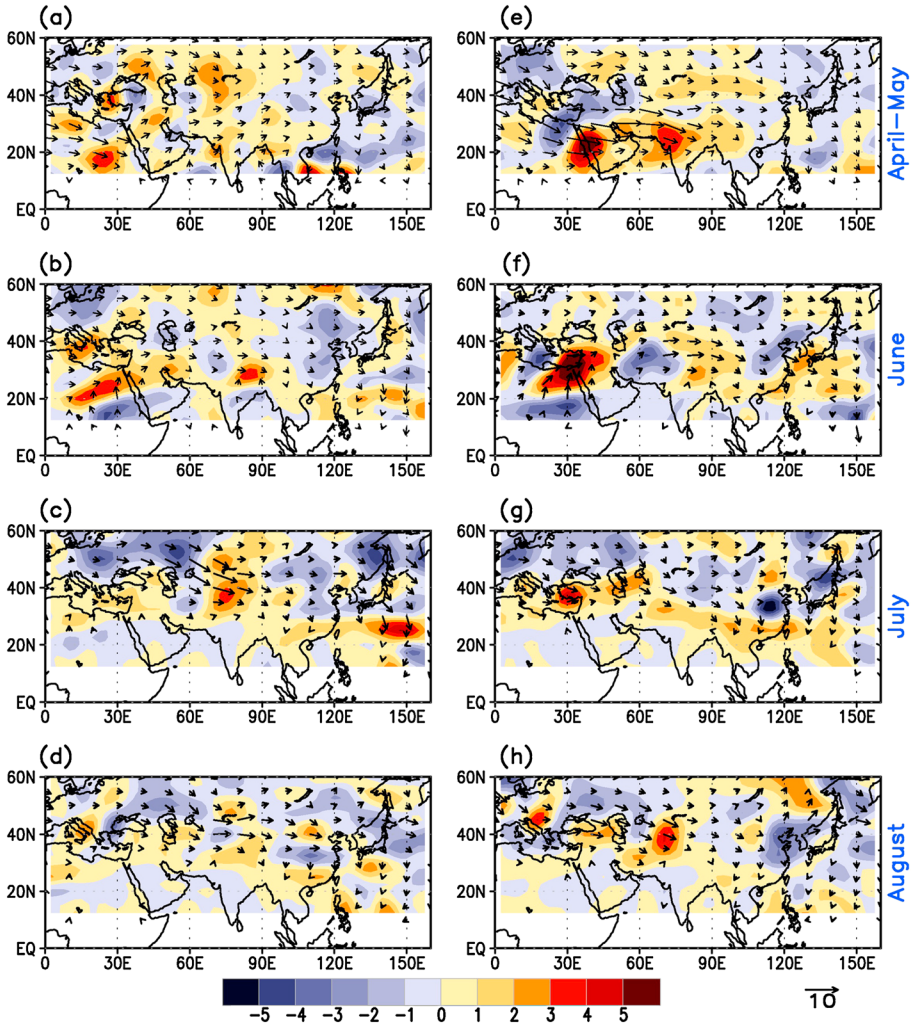

Figure 8. Horizontal wave activity flux (arrows, $m^2 s^{-2}$) and divergence of wave activity flux (shaded, contour interval $10^{-6} m s^{-2}$) at 200 hPa for (a–d) PRA and (e–h) NRA years composite in preonset, June, July, and August, respectively.

the jet. *Joseph and Srinivasan* [1999] observed a large amplitude stationary Rossby wave train in the upper troposphere during May, through the analysis of 200 hPa wind anomalies, and suggested that the stationary waves are basically large-scale Rossby waves, which are induced by the heating caused by heavy rainfall over BoB. However, the found spatial extent of wave activity flux suggests that stationary eastward propagating Rossby wave is associated with midlatitude dynamics.

5. Discussions and Summary

An observational analogy is established to explore the relationship between the preonset (April and May) rainfall and the rainfall of the following monsoon months over the Indian region among various independent data sets. The preonset rainfall has a large variability over northwest India, Pakistan, Afghanistan, southeast Arabia, and Iran, which are climatologically arid regions, and acts as monsoon heat-low region that drives the monsoon winds. The preonset rainfall over the northwest (southeast) region is found to be negatively (positively) correlated with rainfall over India, primarily in the months of June and July, and thereafter the correlation fades gradually in subsequent monsoon months. Non-ENSO year composite clearly depicts that a significant part of early summer monsoon (June and July) rainfall variability (by a maximum of 20%) is associated with the preonset rainfall. The preonset rainfall variability is associated with the low-level mean monsoon circulation and hence rainfall over the Indian region. Low-level wind anomalies suggest that decrease (increase) in rainfall during PRA (NRA) years is associated with

decrease (increase) in the mean monsoon circulation. The preonset rainfall variability over northwest region modulates TTG that helps to sustain the monsoon. A source of wave activity flux is evident to the northwest of India and that flows eastward along 20–30°N over the Indian land region. A common spatial extent in *W* and TTG indicates that buildup of TTG during preonset and in the following months is associated with stationary Rossby wave activity. There are regions of large wave activity flux in the midlatitudes also, which suggest that midlatitude processes too have influence on the rainfall variability. A feedback mechanism has been proposed through which the preonset variability and the following monsoon months rainfall over the Indian region are related. The interaction between preonset condition and following monsoon months rainfall is broadly summarized as follows: as the preonset rainfall over the heat-low region is strongly correlated with the preonset Niño3.4 SST, the anomalous TTG is associated with soil memory and the atmospheric condition through changes in surface heat fluxes. Again the preonset TTG affects the East Asian summer monsoon rainfall during its initial phase, which in turns affects TTG through release of anomalous latent heat. Therefore, a warmer and dryer (colder and wetter) land atmospheric condition over the heat-low region coexists with wet (dry) condition over southeast region of India (i.e., East Asian region). The buildup of TTG since preonset is likely to be due to different factors like surface condition, midlatitude stationary wave activity, and remote influence like ENSO. A poor correlation between Niño3.4 and June-July rainfall over India suggests that there might be indirect role of preonset land atmospheric conditions on ISMR.

The prediction of ISMR is done for the whole season (June–September) using various predictors. However, the first 2 months (June and July) have a large importance in view of agriculture (sowing time), and further the cumulative rainfall of these two months contributes significantly to the seasonal mean. Additionally, the most important predictor having largest influence on ISMR (i.e., ENSO) does not have substantial influence on the starting phase of the monsoon. Thus, the prediction of rainfall in these two months has a lot of implications. Therefore, incorporation of this newly found link in a forecast system may enhance the overall predictability of ISMR, particularly in the months of June and July. The found relation appears to be an intrinsic mode of variability, which has relatively shorter time period as compared to ENSO or IOD. Nevertheless, it has potential to further enhance the ISMR predictability.

Acknowledgments

All the data sets used for this paper are available in the supporting information file. Freeware Ferret and GrADS are used extensively in this study. We sincerely thank Director IITM for all supports and encouragements to carry out this work and D.R. Sikka for scientific discussion, which improved the manuscript. Authors also thank three anonymous reviewers for their constructive comments, which improved the earlier version of this manuscript.

References

Abe, M., A. Kitoh, and T. Yasunari (2003), An evolution of the Asian summer monsoon associated with mountain uplift: Simulation with the MRI atmosphere–ocean coupled GCM, *J. Meteorol. Soc. Jpn.*, *81*, 909–933.

Adler, R. F., et al. (2003), The version 2 global precipitation climatology project (GPCP) monthly precipitation analysis (1979–present), *J. Hydrometeorol.*, *4*, 1147–1167.

Bamzai, A. S., and J. Shukla (1999), Relation between Eurasian snow cover, snow depth, and the Indian summer monsoon: An observational study, *J. Clim.*, *12*, 3117–3132.

Bollasina, M. A., and Y. Ming (2013), The role of land-surface processes in modulating the Indian monsoon annual cycle, *Clim. Dyn.*, *41*, 2497–2509.

Dirmeyer, P. A., X. Gao, M. Zhao, Z. Guo, T. Oki, and N. Hanasaki (2006), GSWP-2 - Multi- model analysis and implications for our perception of the land surface, *Bull. Am. Meteorol. Soc.*, *87*, 1381–1397.

Douville, H., F. Chauvin, S. Planton, J.-F. Royer, D. Salas-Melia, and S. Tyteca (2002), Sensitivity of the hydrological cycle to increasing amounts of greenhouse gases and aerosols, *Clim. Dyn.*, *20*, 45–68.

Ferranti, L., J. M. Slingo, T. N. Palmer, and B. J. Hoskins (1999), The effect of land-surface feedbacks on the monsoon circulation, *Q. J. R. Meteorol. Soc.*, *125*, 1527–1550.

Findlater, J. (1969), A major low-level air current near the Indian Ocean during the northern summer, *Q. J. R. Meteorol. Soc.*, *95*, 362–380.

Goswami, B. N., and R. S. Ajayamohan (2001), Intraseasonal oscillation and interannual variability of the Indian summer monsoon, *J. Clim.*, *14*, 1180–1198.

Goswami, B. N., and P. K. Xavier (2005), Dynamics of internal interannual variability of the Indian summer monsoon in a GCM, *J. Geophys. Res.*, *110*, D24104, doi:10.1029/2005JD006042.

Goswami, B. N., V. Venugopal, D. Sengupta, M. S. Madhusoodanan, and P. K. Xavier (2006), Increasing trend of extreme rain events over India in a warming environment, *Science*, *314*, 1442–1445.

Halley, E. (1686), An historical account of the trade winds, monsoons, observable in the seas between and near the tropics, with an attempt to assign physical cause to said winds, *Philos. Trans. R. Soc. London*, *16*, 153–168.

Harris, I., P. D. Jones, T. J. Osborn, and D. H. Lister (2014), Updated high-resolution grids of monthly climatic observations—The CRU TS3.10 dataset, *Int. J. Climatol.*, *34*, 623–642, doi:10.1002/joc.3711.

Huffman, G. J., R. F. Adler, D. T. Bolvin, G. Gu, E. J. Nelkin, K. P. Bowman, Y. Hong, E. F. Stocker, and D. B. Wolff (2007), The TRMM multi-satellite precipitation analysis: Quasi-global, multi-year, combined-sensor precipitation estimates at fine scale, *J. Hydrometeorol.*, *8*, 38–55.

Joseph, P. V., and J. Srinivasan (1999), Rossby waves in May and the Indian summer monsoon rainfall, *Tellus A*, *51*(5), 854–864.

Kalnay, E., et al. (1996), The NCEP/NCAR 40-year reanalysis project, *Bull. Am. Meteorol. Soc.*, *77*, 437–471, doi:10.1175/1520-0477(1996)077<0437:TNYRP>2.0.CO;2.

Koster, R. D., et al. (2004), Regions of strong coupling between soil moisture and precipitation, *Science*, *305*, 1138–1140.

Kothawale, D. R., and J. R. Kulkarni (2014), Performance of August–September Indian monsoon rainfall when June–July rainfall is reported as being in deficit/excess, *Meteorol. Atmos. Phys.*, doi:10.1007/s00703-014-0353-1.

Kripalani, R. H., and A. Kulkarni (1999), Climatology and variability of historical Soviet snow depth data: Some new perspectives in snow-Indian monsoon teleconnections, *Clim. Dyn.*, *15*, 475–489.
Krishna Kumar, K., B. Rajagopalan, and M. Cane (1999), On the weakening relationship between the Indian monsoon and ENSO, *Science*, *284*, 2156–2159.
Li, C. F., and M. Yanai (1996), The onset and interannual variability of the Asian summer monsoon in relation to land sea thermal contrast, *J. Clim.*, *9*, 358–375.
Liebmann, B., and C. Smith (1996), Description of a complete (interpolated) outgoing long- wave radiation dataset, *Bull. Am. Meteorol. Soc.*, *77*, 1275–1277.
Meehl, G. A. (1997), The South Asian Monsoon and the Tropospheric Biennial Oscillation, *J. Clim.*, *10*, 1921–1943.
Pai, D. S., and S. C. Bhan (2013), Monsoon 2012: A report, IMD Met. Monograph, Synoptic Meteorology 13/2013, NCC.
Parthasarathy, B., R. Kumar, and A. A. Munot (1992), Surface pressure and summer monsoon rainfall over India, *Adv. Atmos. Sci.*, *9*, 359–366.
Prakash, S., A. K. Mitra, I. M. Momin, E. N. Rajagopal, S. Basu, M. Collins, A. G. Turner, K. Achuta Rao, and K. Ashok (2014), Seasonal intercomparison of observational rainfall datasets over India during the southwest monsoon season, *Int. J. Clim.*, doi:10.1002/joc.4129.
Prasanna, V., and T. Yasunari (2009), Time-space characteristics of seasonal and interannual variations of atmospheric water balance over South Asia, *J. Meteorol. Soc. Jpn.*, *87*, 263–287.
Rajeevan, M., J. Bhate, J. D. Kale, and B. Lal (2006), High resolution daily gridded rainfall data for Indian region: Analysis of break and active monsoon spells, *Curr. Sci.*, *9*(3), 296–306.
Ramage, C. S. (1966), The summer atmospheric circulation over the Arabian Sea, *J. Atmos. Sci.*, *23*, 144–150.
Rasmusson, E., and T. H. Carpenter (1983), The relationship between eastern equatorial Pacific Sea surface temperature and rainfall over India and Sri Lanka, *Mon. Weather Rev.*, *111*, 517–528.
Reynolds, R. W., N. A. Rayner, T. M. Smith, D. C. Stokes, and W. Wang (2002), An improved in situ and satellite SST analysis for climate, *J. Clim.*, *15*, 1609–1625.
Robock, A., M. Mu, K. Vinnikov, and D. Robinson (2003), Land surface conditions over Eurasia and Indian summer monsoon rainfall, *J. Geophys. Res.*, *108*, 4131–4143, doi:10.1029/2002JD002286.
Rodwell, M. J., and B. Hoskins (1966), Monsoons and the dynamics of deserts, *Q. J. R. Meteorol. Soc.*, *122*, 1385–1404.
Saha, S. K., S. Halder, K. K. Kumar, and B. N. Goswami (2011), Pre-onset land surface processes and 'internal' interannual variabilities of the Indian summer monsoon, *Clim. Dyn.*, *36*, 2077–2089.
Saha, S. K., S. Halder, A. S. Rao, and B. N. Goswami (2012), Modulation of ISOs by land-atmosphere feedback and contribution to the interannual variability of Indian summer monsoon, *J. Geophys. Res.*, *117*, D13101, doi:10.1029/2011JD017291.
Saha, S. K., S. Pokhrel, and H. S. Chaudhari (2013), Influence of Eurasian snow on Indian summer monsoon in NCEP CFSv2 freerun, *Clim. Dyn.*, *41*, 1801–1815.
Saji, N. H., B. N. Goswami, P. N. Vinayachandran, and T. Yamagata (1999), A dipole mode in the tropical Indian Ocean, *Nature*, *401*, 360–363.
Shinoda, M., and M. Gamo (2000), Interannual variations of boundary layer temperature over the African Sahel associated with vegetation and the upper troposphere, *J. Geophys. Res.*, *105*(D10), 12,317–12,327, doi:10.1029/2000JD900048.
Shukla, J., and Y. Mintz (1982), Influence of land-surface evapotranspiration on the Earth's climate, *Science*, *215*, 1498–1501.
Shukla, J., and D. A. Paolino (1983), The Southern Oscillation and long-range forecasting of the summer monsoon rainfall over India, *Mon. Weather Rev.*, *111*, 1830–1837.
Sikka, D. R. (1980), Some aspects of the large-scale fluctuations of summer monsoon rainfall over India in relation to fluctuations in the planetary and regional scale circulation parameters, *Proc. Ind. Acad. Sci. (Earth Planet Sci.)*, *89*, 179–195.
Sikka, D. R. (1997), Desert climate and its dynamics, *Curr. Sci.*, *72*, 35–46.
Singh, D., C. V. V. Bhadram, and G. S. Mandal (1995), New regression model for Indian summer monsoon rainfall, *Meteorol. Atmos. Phys.*, *55*, 77–86.
Smith, T. M., R. Reynolds, T. C. Peterson, and J. Lawrimore (2008), Improvements to NOAA's historical merged land-ocean surface temperature analysis (1880–2006), *J. Clim.*, *21*, 2283–2296.
Takata, K., K. Saito, and T. Yasunari (2009), Changes in the Asian monsoon climate during 1700–1850 induced by preindustrial cultivation, *Proc. Natl. Acad. Sci. U.S.A.*, *106*, 9586–9589.
Takaya, K., and H. Nakamura (1997), A formulation of a wave-activity flux for stationary Rossby waves on a zonally varying basic flow, *Geophys. Res. Lett.*, *24*, 2985–2988, doi:10.1029/97GL03094.
Takaya, K., and H. Nakamura (2001), A formulation of a phase-independent wave-activity flux for stationary and migratory quasi-geostrophic eddies on a zonally varying basic flow, *J. Atmos. Sci.*, *58*, 608–627.
Ueda, H., and T. Yasunari (1998), Role of warming over the Tibetan Plateau in early onset of the summer monsoon over the Bay of Bengal and the South China Sea, *J. Meteorol. Soc. Jpn.*, *7*, 1–12.
Walsh, J. E., W. H. Jasperson, and B. Ross (1985), Influence of snow cover and soil moisture on monthly air temperature, *Mon. Weather Rev.*, *113*, 756–768.
Webster, P. J. (1983), Mechanisms of monsoon low-frequency variability: Surface hydrological effects, *J. Atmos. Sci.*, *40*, 2110–2124.
Yatagai, A., K. Kamiguchi, O. Arakawa, A. Hamada, N. Yasutomi, and A. Kitoh (2012), APHRODITE: Constructing a long-term daily gridded precipitation dataset for Asia based on a dense network of rain gauges, *Bull. Am. Meteorol. Soc.*, doi:10.1175/BAMS-D-11-00,122.1.